Bull. Chem. Soc. Ethiop. **2025**, 39(1), 165-176.
DOI: https://dx.doi.org/10.4314/bcse.v39i1.14

ISSN 1011-3924
Printed in Ethiopia
Online ISSN 1726-801X

THERMODYNAMIC STUDY OF PYRIDOXINE IN DIFFERENT SOLVENTS AND TEMPERATURES: DFT STUDY

Khalil B. Rasho* and Fanar M. Al-Healy

Department of Chemistry, College of Sciences, University of Mosul, Mosul, Iraq

(Received May 8, 2024; Revised September 20, 2024; Accepted September 23, 2024)

ABSTRACT. The equivalent conductivities (Λ) of B_6 vitamin (pyridoxine) in H_2O and MeOH were measured at different temperatures between 293 to 313 K, as well as in mixtures of H_2O and MeOH at percentages of 10, 20, 30, 40, and, 50% MeOH at 310 K. All the practical results were mathematically processed using the Lee Wheaton equation, which is applied to the derived conductivity of electrolytes with a similar composition (1:1). This equation calculates various conductivity components, including the equivalent conductance at infinite dilution (Λ_o), the ionic conductivity, the distance between ions (R), and also the constant of ionic aggregation (K_a) at best-fit values of (σΛ). The values of these parameters differed from one solvent to another depending on the molecular interactions in the solution and the physical properties of the solvents, such as viscosity and dielectric constant. Finally, thermodynamic quantities for the ion association reaction (ΔG°, ΔH°, and ΔS°) were also studied. Density functional theory (DFT) calculations (B3LYP/6-31G (d,p)) were employed to analyze vitamin B_6 in the gas phase and diverse solvents. Three different continuum methods, namely AM1, PM3, and HF, were utilized, followed by DFT. The final method was utilized to explore the effects on its characteristics.

KEY WORDS: Electrical conductivity, Lee-Wheaton equation, Theoretical chemistry, DFT.

INTRODUCTION

B_6 vitamin (pyridoxine) is a water-soluble vitamin that forms colorless crystals at room temperature. It was discovered in the 1930s [1] and has the nomenclature 4,5-bis(hydroxymethyl)-2-methylpyridin-3-ol with its the chemical structure shown in Scheme 1 [2].

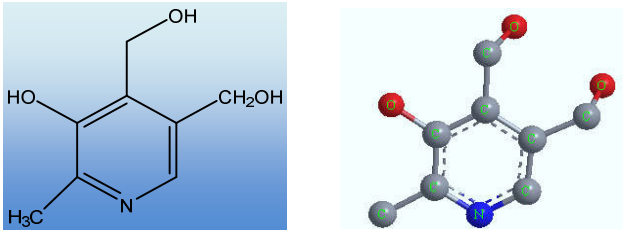

Scheme 1. 2D and 3D structure of pyridoxine.

Vitamin B_6 exists in several forms, including pyridoxine, pyridoxal, pyridoxamine, and their phosphorylated derivatives. However, the most common and stable form is pyridoxine [3]. It acts as a cofactor for participating in the catalytic reactions of numerous enzymes and supports immune and nervous systems, and also plays an important role in the metabolism of amino acids and the conversion of tryptophan to niacin [4].

*Corresponding authors. E-mail: khalil93barakat@gmail.com

Many studies have been conducted on this vitamin, using different chemical methods and techniques to analyze its structure, which contains several functional groups on the pyridine ring. Some studies have attempted to link the electrochemical signals that are emitted to the functional groups possessed by the pyridine ring. In recent years, there has been increasing interest in this vitamin through electrochemical studies due to its electrically active functional groups. These techniques include chromatographic methods. The technique demonstrated a strong linear range for vitamin B_6 analysis, with a LOD of 0.025 μg mL^{-1} [5]. The outcome results showed that vitamin B_6 could be estimated both qualitatively and quantitatively using this approach. Pyridoxine hydrochloride, or vitamin B_6, has been measured using the spectrophotometric technique for both its pure form and its pharmaceutical formulations. The main process of the recommended approach is the coupling reaction of diazotized metoclopramide hydrochloride with pyridoxine hydrochloride in an alkaline medium, which results in the formation of a vivid yellowish orange azo dye that is stable and soluble in water [6]. The utilization of environmentally friendly nanoporous natural zeolite exchanged with Ni^{2+} ions (NiZ) and conductive carbon black (CB) in the fabrication of a novel and selective voltammetric sensor of vitamin B_6 (VB_6) is presented [7]. The zinc ferrite nano-particles ($ZnFe_2O_4$) modified screen-printed graphite electrode ($ZnFe_2O_4$/SPGE) was used for the voltammetric determination of vitamin B_6 in real samples, using differential pulse voltammetry (DPV) vitamin B_6 sensor with a linear range from 0.8 to 585.0 μM and a detection limit of 0.17 μM. Under isocratic conditions using high-performance liquid chromatography (HPLC), and UV detection at 290 nm, the $ZnFe_2O_4$/SPGE sensor shows good resolution between the voltammetric peaks of vitamin B_6 and vitamin C. This allows for effective analysis for vitamin B_6 in commercial aqueous nutritional drinks and solid tablets [8, 9]. MXenes are 2D nanomaterials known for their high electrical conductivity, strong biocompatibility, and ease of functionalization, making them as materials for the future generation. This study presents the first electrochemical detection of vitamin B_6 utilizing the brush-coated carbon fiber paper electrode (MnO_2-Pi/MXene/CFP), which is made of manganese dioxide and inorganic phosphate [10]. Iron oxide nanoparticles (IONs) combined with reformed carbon paste (CP) provide a straightforward, highly sensitive electrochemical sensor. This sensor was designed to detect vitamin B_6, a critical medication, in phosphate buffer solution (PBS) with a pH range of 5.0 to 8.0 [11]. Roanalytical food sensors using radioanalysis that are based on amplifying carbon paste electrodes (CPE), nanocomposite NiO-CNTs, 1-methyl-3-octylimidazolium hexafluorophosphate (MOHFPE), and others [12]. Vitamin B_6 is important for good health, so obtaining adequate amounts of this vitamin is essential. The amount set by the United States Food and Nutrition Board, which was 100 mg per day, is obtained by eating foods, especially of plant and animal origin, such as vegetables, nuts, and meat [13]. Not only is it alone, but its derivatives also have an important role in stimulating enzymes and processes. Metabolism within the human body, as well as biological activity, and in addition to its other functions, it works as a coenzyme in metabolic processes. Therefore, we notice that when investigating this vitamin, clear effects appear on the metabolic work of the individual, and many diseases associated with this vitamin appear. Vitamin B_6 derivatives enter in the unphosphorylated form and are phosphorylated in the cell [14].

Electrochemistry is the branch of science that studies the chemical effects caused by the passing of an electrical current. It explores the relationship between the amount of applied electricity and the amount of substance precipitated or liberated, as described by Faraday laws of electrolysis. One of the early applications of electrochemistry was determining the solubility of materials, association constants, and other thermodynamic parameters. Conductivity measures the ability of a substance to transfer electrical charge, whether through ions or electrons, in response to an applied voltage. The conductivity measurement was done based on the equation of Kohlrausch, which was instrumental in developing precise methods for conductivity measurement. After analyzing the output data using the LW conductivity equation, the Λ_o and K_a were derived. The equivalent ionic conductivity (Λ_o) was obtained using literature values for the

conversion number, which limits the cation to (K^+) within the same temperature range. The activation enthalpy of the ionic movement, along with the thermodynamic variables (ΔG, ΔH, and ΔS) for the ion-association reaction, were computed and analyzed in relation to the ionic size, viscosity, permittivity, structure, and basicity [15]. Computational chemistry is a rapidly developing branch of theoretical chemistry and its applications that are constantly and rapidly expanding. It studies the properties of molecules to understand the properties of materials. By understanding of the properties of materials, we can better predict the characteristics of materials that have not yet been synthesized [16]. The molecular electronic structure of compounds was optimized by quantum chemical computations (molecular geometry structure optimization, and HOMO-LUMO studies), which was done by the DFT/B3LYP method at the 6-31G (d, p) basis set to confirm experimental data. Density Functional Theory (DFT) is a theoretically rigorous yet practically empirical method for addressing the many-electron problem in fermionic systems. This approach is foundational in chemistry, biology, and physics. By combining it with a mixed quantum-classical approach for the nuclei, such as molecular dynamics or harmonic approximations for the potential energy surface, DFT can effectively tackle numerous obstacles in (bio)chemistry and physics, providing valuable insights with satisfactory accuracy. The intricate theoretical and technical aspects of DFT have been thoroughly examined and extensively deliberated upon in a comprehensive open discussion review. Such applications often involve assessing the viability of structures and reaction mechanisms proposed by synthetic chemists. Additionally, they involve the visualization of frontier orbitals, as well as the determination of ƐHOMO and ƐLUMO, to interpret electrochemical experiments within the realm of materials science [17].

EXPERIMENTAL

Conductivity measurement

The conductivity of pyridoxine was measured, in H_2O, and MeOH, and their mixture using a WTW Inolab 740 computerized conductivity meter (Therminal740, 2003, Made in Germany) [18]. A weight of 0.000169 g of pyridoxine (manufactured by BDH) was measured using Sartoins (5dis) (1995) MP, and dissolved in 10 mL of different solvents (water, methanol, and a mixture of methanol and water with different percentages: 10, 20, 30, 40 and 50%) with several additions of stock solution. To add the stock solution into the cell of the conductometer, a 1 mL syringe was used. The stock solution was prepared by weighing with freshly prepared solvents. The first step in measuring the conductivity involved adding a known quantity of solvent into a dry, clean and pre-weighed conductivity cell, which was then connected to a water circulation thermostat to control the temperature of the cell and its contents. A stirrer was used to mix and homogenize the solution after each addition, before recording the conductivity. The Conductivity of pyridoxine was measured at different temperatures (20, 25, 30, 35 and 40 °C) in water and methanol, while the conductivity of the mixture was measured at 310 K. After the completion of all additions, the cell was dried and reweighed to determine any change in weight, and it was found that the loss was not more than 0.02%.

Quantum chemical computations

The chemistry program, Chem 3DChemBioOffice software version 16.0 (level: Ultra) was used to perform theoretical calculations on the molecule by applying the semi-empirical methods (AM1, PM3, HF), Finally, calculations were made based on the DFT at B3LYP level with a 6-31G (d,p), and the energy minimization of the molecule was performed, and then the HOMO and LUMO energy values were calculated after reaching the lowest energy level for the molecule, and through these values, many theoretical descriptions of the molecule are obtained [19].

RESULTS AND CALCULATION

Conductivity measurements of pyridoxine

The Kohlrausch equation was used to identify the types of pyridoxine electrolytes by plotting the relation between equivalent conductivity (Λ) against the square root of concentration ($\sqrt{C}$) in different solvents and temperatures. A special calculation program was used to determine Λ by inputting the conductivity results and relevant physical parameters, at different temperatures, along with the weights of the additives [20]. In these solutions, the positive ion is M^+ and the negative ion is X^-, the equation for these solutions can be explained Equation 1:

$$MX_{aq} \overset{K_a}{\rightarrow} M^{+}_{aq} + X^{-}_{aq} \quad (1)$$

where K_a: association constant.

This relation established that the solution exhibits weak electrolyte behavior, as determined by electrical conductivity taken at different temperatures of the solution and in all solvents. Pyridoxine behaves as a symmetrical electrolyte of 1:1 type. The data presented in tables 1A, 1B, and 1C, and Fgure 1 show the behavior of pyridoxine.

Table 1A. Equivalent conductivities (Λ) of pyridoxine as a function of the square root of concentration √Conc. at 293 to 313 K in H_2O.

Conc. (mol/L) 10^{-6}	$\sqrt{C}$ (mol/L) 10^{-4}	Λ ($\Omega^{-1}.\Lambda^{-1}.cm^2$) 293 K	Λ ($\Omega^{-1}.\Lambda^{-1}.cm^2$) 298 K	Λ ($\Omega^{-1}.\Lambda^{-1}.cm^2$) 303 K	Λ ($\Omega^{-1}.\Lambda^{-1}.cm^2$) 308 K	Λ ($\Omega^{-1}.\Lambda^{-1}.cm^2$) 313 K
0.54	7.33	464.7029	461.0567	496.3219	494.0770	625.6672
1.05	10.25	285.1938	291.0303	272.3278	241.9025	355.1613
1.52	12.32	230.2732	249.0039	217.0641	187.4385	250.2020
2.02	14.22	197.8176	216.8081	180.3182	162.7957	226.3210
2.52	15.86	178.7132	194.7179	177.1774	150.4868	210.1824
2.95	17.16	178.2607	187.8558	164.7851	147.4943	191.9882
3.46	18.61	165.9562	175.9460	156.4291	142.9797	180.1847
3.94	19.85	171.1881	173.1456	158.4584	138.6951	171.0052
4.41	21.01	169.8921	165.7725	155.2428	139.8298	164.9904
4.86	22.04	174.9027	166.865	146.7871	133.5376	165.8477
5.21	22.83	172.6279	159.4849	147.2309	133.1855	157.9205
5.67	23.80	172.0413	160.7695	147.9093	132.1338	155.0590
6.13	24.75	167.3042	156.7847	145.3262	126.9252	155.6389
6.63	25.75	165.8302	155.2312	144.8664	129.2996	152.7229

Table 1B. Equivalent conductivities (Λ) of pyridoxine as a function of √Conc. at a temperature ranging from293 to 313 K in MeOH.

Conc. (mol/L) 10^{-6}	$\sqrt{C}$ (mol/L) 10^{-4}	Λ ($\Omega^{-1}.\Lambda^{-1}.cm^2$) 293 K	Λ ($\Omega^{-1}.\Lambda^{-1}.cm^2$) 298 K	Λ ($\Omega^{-1}.\Lambda^{-1}.cm^2$) 303 K	Λ ($\Omega^{-1}.\Lambda^{-1}.cm^2$) 308 K	Λ ($\Omega^{-1}.\Lambda^{-1}.cm^2$) 313 K
0.52	7.23	287.3325	335.2807	345.95	348.2144	342.3256
1.04	10.18	168.7047	206.3128	207.5812	195.3688	200.8476
1.56	12.51	127.8875	161.8415	155.2227	149.6562	157.1078
2.08	14.41	108.3188	132.4125	130.8393	126.221	132.0669
2.59	16.08	96.63583	114.9688	115.2009	110.6547	114.781
3.06	17.5	89.83664	104.7191	104.7452	100.6954	104.8115
3.52	18.77	85.19514	96.6487	97.63762	93.92256	97.98969
4.02	20.05	80.82598	91.66313	92.33327	88.93501	91.10464
4.52	21.25	77.49113	87.18339	88.12503	90.47591	92.77539
4.93	22.2	81.15218	83.90997	89.68638	91.90251	94.78123
5.48	23.41	82.13113	80.55179	85.67187	87.81229	95.19334
5.95	24.4	84.00467	78.23381	83.4041	85.3741	95.98158
6.41	25.31	85.82818	76.47159	85.27065	87.09817	97.22127
6.83	26.14	84.14501	75.15405	87.20071	88.46799	98.40324

Table 1C. Equivalent conductivities (Λ) of pyridoxine as a function of √Conc. at 310 K in different percentages of the mixture.

Conc. (mol/L) 10^{-6}	$\sqrt{C}$ (mol/L) 10^{-4}	Λ ($\Omega^{-1}.\Lambda^{-1}.cm^2$) 10%	Λ ($\Omega^{-1}.\Lambda^{-1}.cm^2$) 20%	Λ ($\Omega^{-1}.\Lambda^{-1}.cm^2$) 30%	Λ ($\Omega^{-1}.\Lambda^{-1}.cm^2$) 40%	Λ ($\Omega^{-1}.\Lambda^{-1}.cm^2$) 50%
0.59	7.72	377.3828	365.0209	329.1327	343.2444	337.6159
1.08	10.4	277.4105	313.1211	234.4471	203.567	226.2108
1.59	12.62	235.5531	279.5286	194.2596	159.0689	171.3693
2.09	14.45	215.3838	250.4302	175.3251	133.1595	140.8322
2.61	16.14	211.079	229.5942	163.5052	135.3913	122.709
3.02	17.37	215.5171	219.1053	157.8992	129.3918	119.2178
3.52	18.77	226.9543	211.3601	151.4315	132.7651	117.7813
4.00	20	231.2356	212.8783	149.1207	136.5448	109.6849
4.44	21.07	225.2271	211.354	152.7794	137.9328	110.4875
4.92	22.19	218.2956	210.8483	155.4965	133.6744	109.8714
5.49	23.43	209.4454	202.5347	155.0798	133.887	103.2447
5.92	24.34	211.0699	196.279	152.8149	131.4895	99.30814
6.35	25.2	208.5807	206.0223	150.452	129.7386	96.89278
6.81	26.09	205.6501	210.3787	149.2893	127.7748	92.70698

By using different solvents and temperatures, it was noticed that that as the temperature increased, the conductivity values also increased. This indicates that with higher temperatures, ions gain more energy, enhancing their ability to transfer charge and thus increasing the conductivity [21]. In addition, the dielectric constant of solvents affects the conductivity value. As the number of free ions increases, the electrical conductivity also increases. [22]. The LW equation was applied to calculate the Equivalent conductivities (Λ), association constant (K_a), and the distance between R (Å) and σΛ of pyridoxine solution described above. A specialized program was used to perform the analysis, using a specific analysis software after providing it with measurement data, such as fixed cell concentrations (0.5 cm), concentration, equivalent conductivity values and physical parameters such as density, viscosity and dielectric constant of the solution, all of which depend on changes in temperature and solvent. Table 2 shows values of K_a, Λ, R, and σΛ of pyridoxine.

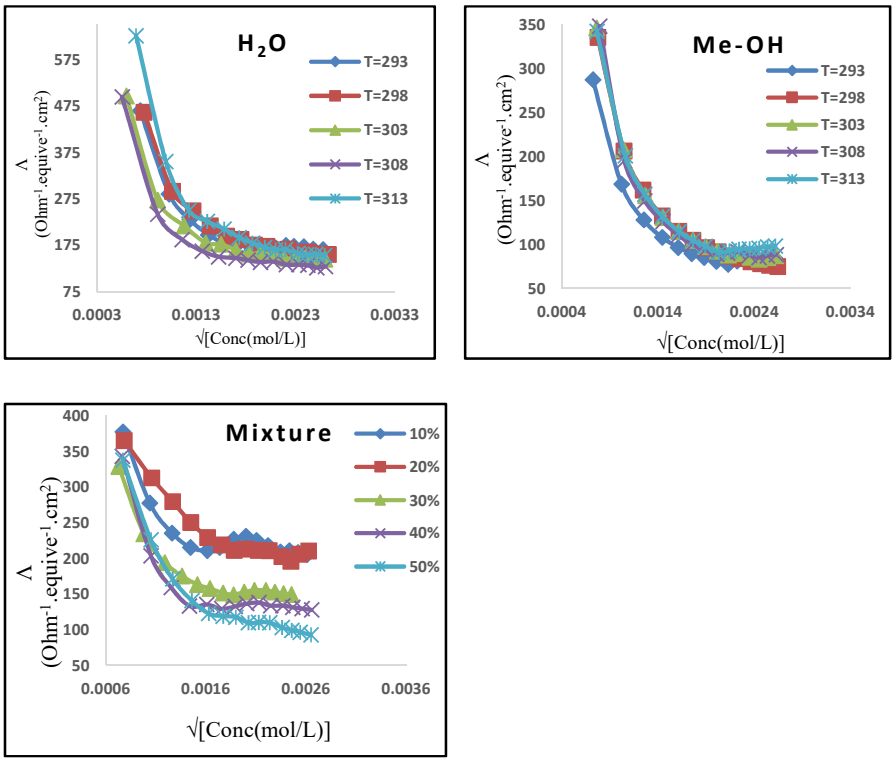

Figure 1. Equivalent conductivities (Λ) of pyridoxine as a function of √Conc. at 310 K in different solvents and temperatures.

Table 2. K_a, Λ, R (Å) and σΛ of pyridoxine at different temperatures in H_2O, MeOH, and mixtures.

Water				
T (K)	K_a	Λ_o(Ohm^{-1}.equive^{-1}.cm^2)	R (Å)	δΛ
293	1399696	537.643	1	0.31
298	3628520	795.443	1	0.20
303	4077069	737.264	1	0.26
308	4209053	679.693	1	0.30
313	1627341	580.789	1	0.57
Methanol				
T(K)	K_a	Λ_o(Ohm^{-1}.equive^{-1}.cm^2)	R (Å)	δΛ
293	1933711	333.060	1	0.22
298	5267053	472.230	1	0.06
303	2127093	359.304	1	0.10
308	1000983	294.007	1	0.44
313	1237861	329.084	1	0.31
Mixture				
%	K_a	Λ_o(Ohm^{-1}.equive^{-1}.cm^2)	R (Å)	δΛ
10	164133	325.244	1	0.24

20	364522	400.348	1	0.13
30	718665	351.136	1	0.18
40	588050	304.701	1	0.29
50	3564444	158.063	1	0.20

The results show that a cation is associates with an anion to form a contact ion–pair (CIP), as evidenced by the distance between the cation and anion is less than 2 Å. The standard deviation confirms that this equation is appropriate for the study.

Thermodynamic study

The Vant-Hoff equation, eq. No. 1, was used to determine the thermodynamic parameters [23]. Plotting ln(K_a) against 1/T is shown in Figure 2.

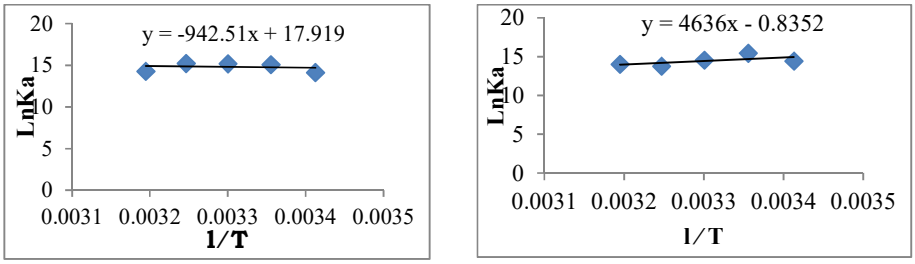

Figure 2. The relation between ln(k_a)and $\frac{1}{T}$ of pyridoxinein water and methanol.

The relation gives a straight line of pyridoxine solutions. The values of ΔH were determined from the slope of Equation 2, the ΔG and ΔS values:

$$\mathrm{LnKa} = -\frac{\Delta H}{RT} + C \quad (2)$$

$$\Delta G = -RTLnKa$$

$$\Delta G = \Delta H\text{-}T\,\Delta S$$

Table 3. Thermodynamic parameters of pyridoxine.

Water					
T (K)	(1/T)(K^{-1})	ΔS ($J.mol^{-1}.K^{-1}$)	ΔG ($kJ.mol^{-1}$)	ΔH ($kJ.mol^{-1}$)	LnK_a
293	0.003413	144.41	-34.47	7.836	14.15
298	0.003356	151.88	-37.42		15.10
303	0.003300	152.41	-38.34		15.22
308	0.003247	152.26	-39.06		15.25
313	0.003195	143.95	-37.22		14.30
Methanol					
T (K)	(1/T)(K^{-1})	ΔS ($J.mol^{-1}.K^{-1}$)	ΔG ($kJ.mol^{-1}$)	ΔH ($kJ.mol^{-1}$)	LnKa
293	0.003413	-11.20	-35.26	-38.54	14.47
298	0.003356	-0.66	-38.34		15.48
303	0.00330	-6.07	-36.70		14.57
308	0.003247	-10.27	-35.38		13.82
313	0.003195	-6.50	-36.51		14.03

The tables display that the dissociation is endothermic because the values of ΔH (enthalpy of association) in water are (+ve), the reaction was spontaneous, and the values of ΔG (Gibbs free energy) are (-ve). The regulation of the system as a result of association under the influence of solvation and the columbic effect in spontaneous continuum media is indicated by the positive values of ΔS [24].

Walden product

We used Walden equation to calculate The walden product ($\Lambda^{o}\eta$) for the studied pyridoxine.

$$\eta\,\Lambda^{\circ} = constant$$

The mixture of methanol in water was obtained by multiplying each value of Λ_o from Table 2 by the viscosity (η) at 310 K [25]. The effect of viscosity and density at different percentages is illustrated. All resulting data are listed in Table 4.

Table 4. The percentage of methanol in water with ηΛ.

Percentage %	η		Λ_o at 310 K	ηΛ
10	0.00109		325.244	0.356
20	0.00150		400.348	0.6
30	0.00190		351.136	0.669
40	0.00231		304.701	0.704
50	0.00271		158.063	0.431

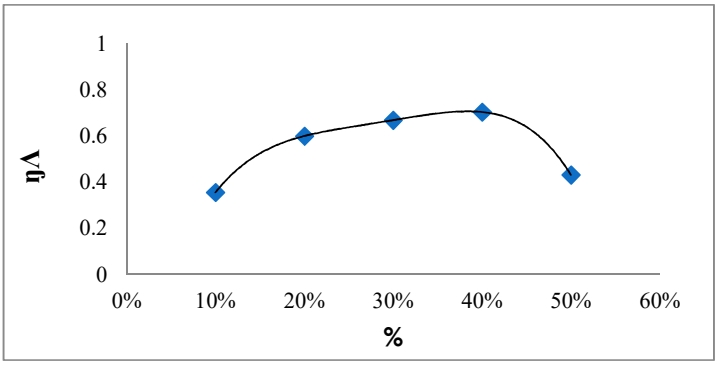

Figure 3. The relation between the percentage of methanol in water against ηΛ.

Theoretical discussion

Chemical Reactivity Theory, also known as Conceptual Density Functional Theory (DFT), is a powerful tool for analyzing, interpreting, and forecasting the results of chemical interactions. In this study, density functional theory (DFT) and thermodynamics modeling were used to compute several molecule descriptors and properties of their ideal geometries. Table 5 lists the theoretical methodologies used to find the minimal energy [26].

Table 5. The energy values of each approach used in theoretical calculation.

	Gas phase				Water	Methanol
	AM1	PM3	HF	DFT	DFT	DFT
Finished energy kcal/mol	-117.83	-122.66	-369026.9	-371287.88	-371299.82	-371299.57
ε_{HOMO}	-0.40227	-0.38289	-0.46733	-0.28760	-0.29304	-0.29298
ε_{LUMO}	-0.00896	-0.01554	0.10425	-0.03099	-0.03929	-0.03919

Physio-chemical descriptors play a crucial role in comprehending the reactivity of a molecule or system, and they are determined by analyzing the energy levels of the HOMO and LUMO. According to literature, the HOMO tends to donate electron density, whereas the LUMO acts as an electron acceptor. The energy gap between the HOMO and LUMO, known as EL-H, is utilized to elucidate the reactivity of the molecules under investigation. Even a slight alteration in stability becomes apparent, when water is used as a solvent. Chemical hardness and softness (S) are employed to assess the reactivity and stability of the molecule or system. It has been noted that higher softness or lower hardness value signifies increased polarization within the molecule or system. All descriptors determined from DFT energies are listed in Table 6 [27].

Table 6. Descriptors calculated from DFT –HOMO, and LUMO energies.

Descriptors/System	Gas	Water	Methanol
HOMO (eV)	-0.2876	-0.2930	-0.2929
LUMO (eV)	-0.0309	-0.0392	-0.0391
GAP (ΔEL-H) (e)	0.2566	0.2537	0.2537
Ionization potential (I)	0.2876	0.2930	0.2929
Electronic affinity (A)	0.0309	0.0392	0.0391
Hardness	0.1283	0.1268	0.1268
Softness	3.89712	3.94322	3.94322
Chemical potential (μ)	-0.1593	-0.1661	-0.1660
Electrophilicity (ω)	0.0988	0.1088	0.1086

After completing the theoretical minimization, compute the properties of the molecule (B_6) in gas, water, and methanol solvents as shown in Table 7. From the values of these descriptors, we can see the solvent effect on them like Connolly parameters, which decreased in the solvents compared to the gas phase system. Also, the molecular volume is one of the important descriptors that varies when the system changes, its value was 1486.683, 1370.281, and 1280.135 in gas, water, and methanol systems, respectively. The highest value is in gas phase because there is no solvent effect on the molecule. This value decreases in water and even more in methanol, indicating that the methanol system is more influenced by the molecular volume. This can be reflected in the equivalent conductivity values at infinite dilution and at a temperature of 298 K (Λ_o). The value in water is higher than in methanol, with Λ_o in water at 298 K = 248.285 $S.eq^{-1}.cm^2$ and Λ_o in methanol at 298 K = 87.158 $S.eq^{-1}.cm^2$. It is also noticeable from the calculated parameter values and their relationship with the practical parameters that the theoretically calculated entropy values are lower in the water and methanol phases compared to the gas phase, which indicates that the solvent molecules affect the B_6 molecule.

Table 7. DFT descriptors of the B6 molecule in three systems.

Descriptors	Gas	Water	Methanol
Lipinski rule	169.074; 4; 3; 2; -0.345	169.074; 4; 3; 2; -0.345	169.074; 4; 3; 2; -0.345
Connolly accessible area (Å^2)	337.444	337.467	337.473
Connolly molecular area (Å^2)	166.935	166.884	166.89
Connolly solvent excluded volume (Å^3)	137.789	137.527	137.541
Number of H bond acceptors	4	4	4
Number of H bond donors	3	3	3
Dipole (Debye)	2.1655	5.2149	5.2088
Molecular volume (Bohr**^{3}/mol	1486.683	1370.281	1280.135
RMS force (kcal/mol)	6.4716	6.9541	6.9407
SCF energy (kcal/mol)	-369038.78	-369042.83	-369042.85
Entropy (cal/mol-Kelvin)	96.255	94.715	94.719
Molecular mass (au)	169.07389	169.07389	169.07389
Thermodynamic energy (kcal/mol)	131.811	132.085	132.088
Zero-point energy (kcal/mol)	125.63294	126.092904	126.095414
Polarizability	123.6712	117.1954	117.1929
Molecular topology descriptors			
Balaban index	26520	26520	26520
Cluster count	12	12	12
Molecular topological index	1314	1314	1314
Num rotatable b	2 Bond(s)	2 Bond(s)	2 Bond(s)
Polar surface area (Å^2)	73.05	73.05	73.05
Radius	3 Atom(s)	3 Atom(s)	3 Atom(s)
Shape attribute	10.0833333333333	10.0833333333333	10.0833333333333
Shape coefficient	1	1	1
Sum of degrees	24	24	24
Sum of valence degrees	44	44	44
Topological diameter	6 Bond(s)	6 Bond(s)	6 Bond(s)
Total connectivity	0.0277777777777778	0.0277777777777778	0.0277777777777778
Total valence connectivity	0.00072168783648703	0.00072168783648703	0.00072168783648703
Wiener index	186	186	186

CONCLUSION

The current study presents conductivity measurements for pyridoxine solutions in water, methanol at varying temperatures, and methanol-water mixtures. The data was analyzed using the Lee-Wheaton equation with the best-fit standard deviation values ($\sigma\Lambda$) for symmetrical electrolytes. The conductivity parameters, including association constant K_a, Λ_o, and distance parameter R, exhibit variations across solvents due to differences in dielectric constant, viscosity, and solution interactions. These physical properties affect the K_a and Λ_o, values, which reflect the thermodynamics parameters. The ΔH value of the compound in water is more than its value in methanol because the K_a value is more in water than in methanol (the K_a value in methanol is not systematically increasing or decreasing). When ΔH and ΔS are positive values, it indicates that

the process is endothermic and more random. A negative ΔG suggests that the process is spontaneous. In addition, the theoretical results show that the effect of the solvent properties on the K_a matches with the experimental results. The difference in the three Conley coefficient values and the molecule's size in relation to the gas phase show that the solvent affects the molecule of a compound. This means that the larger the solvent molecule, the lower the equivalent conductivity value, which impedes movement in the solution. The practically calculated entropy values also show this relationship.

REFERENCES

1. Combs, G.F., Jr.; McClung, J.P. *The Vitamin: Fundamental Aspects in Nutrition and Health*, 5th ed.; Elsevier Inc.: Amsterdam; **2017**; p. 52.
2. Dajana, G.; Spomenka, K.; Valentina, B.; Jasna, V. *The Chemistry and Biochemistry of Vitamin B6: Synthesis of Novel Analogues of Vitamin B6*. *ResearchGate*, **2012**; Chapter 9, p. 136.
3. Ueland, P.M.; McCann, A.; Midttun, Ø.; Ulvik, A. Inflammation, vitamin B6 and related pathways. *Mol. Asp. Med.* **2017**, 53, 10-27.
4. Rison, S.; Mathew, A.T.; George, L.; Maiyalagan, T.; Hegde, G.; Varghese, A. Pt nanospheres decorated graphene-β-CD modified pencil graphite electrode for the electrochemical determination of vitamin B6. *Topics Catal.* **2022**, DOI: https://doi.org/10.1007/s11244-021-01559-1.
5. Patle, T.K.; Sim, K.S. Simultaneous determination of B1, B3, B6, and C vitamins in green leafy vegetables using reverse phase-high performance liquid chromatography. *Microchem. J.* **2022**, 176, 107249.
6. Abdul-Aleem, Z.S.; Abdul-Aleem, Z.R.; Sabeeh, O.N. Spectrophotometric determination of vitamin B6 in pure and pharmaceutical formulations with diazotized metoclopramide hydrochloride. *Int. J. Drug Dev. Tech.* **2021**, 11, 787-792.
7. Radosław, P.; Katarzyna, F.; Bogusław, B. Electrochemical sensor based on Ni-exchanged natural zeolite/carbon black hybrid nanocomposite for determination of vitamin B6. *Microchimica Acta* **2021**, 188, 323.
8. Peyman, M.; Maedeh, J.; Sayed, A. Voltammetric determination of vitamin B6 in the presence of vitamin C based on zinc ferrite nano-particles modified screen-printed graphite electrode. *ADMET & DMPK*, **2023**, 11, 251-261.
9. Bartzatt, R.; Gajmer, P.; Nguygen, M.H.C.; Tran, A.M. *Assay of Vitamin B6 (Pyridoxine Hydrochloride) Utilizing Isocratic Reversed Phase High Performance Liquid Chromatography*, Chapter 2: in *Advances in Applied Science and Technology*, Vol. 3, Tuzemen, S.; Khan, F. (Eds.), **2019**, pp. 12-26. https://doi.org/10.9734/bpi/aast/v3.
10. Rajeev, R.; Cherian, A.; Thadathil, D.; Varghese, A. Electrochemical determination of vitamin B6 using coral-like MnO_2-π on $Ti_3C_2T_x$ MXene. *Mater. Res. Bull.* **2024**, 169, 112523.
11. Moustafa, A.; El Kamel, R.S.; Abdelgawad, S.; Fekry, A.M.; Shehata, M. Electrochemical determination of vitamin B6 (pyridoxine) by reformed carbon paste electrode with iron oxide nanoparticles. *Int. J. Electrochem. Sci.* **2022**, 28, 4471-4484.
12. Sadeghi, H.; Shahidi, S.; Raeisi, S.; Ghorbani, H.; Karimi, F. Electrochemical determination of vitamin B6 in water and juice samples using an electrochemical sensor amplified with NiO/CNTs and ionic liquid. *Int. J. Electrochem. Sci.* **2020**, 15, 10488-10498.
13. Ogunneye, A.L.; Banjoko, O.O.; Gbadamosi, M.R.; Falegbe, O.H.; Moberuagba, K.H.; Badejo, O.A. Spectrophotometric determination of caffeine and vitamin B6 in selected beverages, energy/soft drinks and herbal products. *Niger. J. Basic Appl. Sci.* **2020**, 28, 22-29.
14. Spinneker, A.; Sola, R.; Lemmen, V.; Castillo, M.J.; Pietrzik, K.; González-Gross, M. Vitamin B6 status, deficiency and its consequences - an overview. *Nutr. Hosp.* **2007**, 22, 7-24.

15. Al Lehebe, A.J.M.B.; Al Tamer, M. Electrical conductivity study of aqueous solutions for some complexes of manganese, cobalt, nickel, and copper divalent elements in different temperatures. *Raf. J. Sci*. **2021**, 30, 19-32.
16. Mammino, L. Computational chemistry capacity building in an underprivileged context: challenges, outcomes and perspectives. *Tanz. J. Sci.* **2012**, 38, 95-107.
17. Komasa, A.; Babijczuk, K.; Dega-Szafran, Z.; Gołdyn, M.; Bartoszak-Adamska, E.; Szafran, M.; Cofta, G. Interactions of pyridoxine (vitamin B6) with squaric acid and water: experimental and theoretical studies. *J. Mol. Struct.* **2022**, 1251, 131773.
18. Bursch, M.; Mewes, J.M.; Hansen, A.; Grimme, S. Best-practice DFT protocols for basic molecular computational chemistry. *Angew. Chem. Int. Ed.* **2022**, 61, E202205735.
19. Abdulrahman, Sh.; Al-Healy, F. Electrical conductance and theoretical study of glutamic acid in different solvents at 310.16 k. *Egypt. J. Chem.* **2021**, 64, 4359–4367.
20. Light, T.S. Temperature dependence and measurement of resistivity of pure water. *Anal. Chem.* **1984**, 56, 1138-1142.
21. De Silva, L.D.P.; Freitas, K.H.G.; De Sousa, F.F. Electrical and dielectric properties of water. *Scientia Plena* **2017**, 13. DOI: 10.14808/sci.plena.2017.012722.
22. Lee, W.H.; Wheaton, R.J. Conductance of symmetrical, unsymmetrical, and mixed electrolytes. *J. Chem. Soc. Faraday Trans*. *II* **1978**, 74, 743-766.
23. Al-Healy, F.M.; Hameed, Y.O. Electrochemical and thermodynamic study of tyrosine and its complexes in aqueous solution by conductivity measurement. *EPSTEM* **2019**, 7, 48-57.
24. Nancollas, G.H. *Interactions in Electrolyte Solutions*, Elsevier: Amsterdam; **1966**; Tables A-1 and A-5.
25. Al-Healy, F.; Hameed, Y. Measurement of the electrical conductivity of equivalent a number of aspartic acid complexes in different percentages of water mixture with methanol at 310 absolute temperature. *Raf. J. Sci*. **2020**, 29, 80-94.
26. Shahraki, M.; Dehdab, M.; Elmi, S. Theoretical studies on the corrosion inhibition performance of three amine derivatives on carbon steel: molecular dynamics simulation and density functional theory approaches. *J. Taiwan Inst. Chem. Eng*. **2016**, 62, 313-321.
27. Singh, H.; Singh, A.; Banipal, T.S.; Singh, P.; Bahadur, I. Temperature and concentration dependent physicochemical interactions of l-ascorbic acid in aqueous LiCl solution: experimental and theoretical study. *Colloids Surf.* A **2021**, 623, 126.